JOURNAL OF GUIDANCE, CONTROL, AND DYNAMICS
Vol. 28, No. 3, May–June 2005

Engineering Notes

ENGINEERING NOTES are short manuscripts describing new developments or important results of a preliminary nature. These Notes should not exceed 2500 words (where a figure or table counts as 200 words). Following informal review by the Editors, they may be published within a few months of the date of receipt. Style requirements are the same as for regular contributions (see inside back cover).

Stability Criteria of Slosh Motion with Periodicity in a Spinning Spacecraft

Ja-Young Kang*
Hankuk Aviation University,
Gyeonggi-do 412-791, Republic of Korea
and
John E. Cochran Jr.†
Auburn University, Auburn, Alabama 36849-5338

Nomenclature

a	=	transverse component of the system angular momentum
C_1, C	=	centers of mass of the main body and the system
$\boldsymbol{F}$	=	thrust vector $(0\ \ 0\ \ F_3)^T$ along the symmetry axis passing through C_1
$\boldsymbol{H}$	=	angular momentum vector of the system
I_1, I_2, I_3	=	moments of inertia of the main body about the centroidal principal axes x, y, and z
m_1, m_2	=	masses of spacecraft main body and pendulum bob
$\boldsymbol{O}$	=	pivot point of the pendulum
r	=	length of massless rod connecting the pendulum bob
$\boldsymbol{r}, \boldsymbol{r}_O, \boldsymbol{r}_p$	=	position vectors from $\boldsymbol{O}$ to m_2, C_1 to $\boldsymbol{O}$, and C_1 to m_2
$\boldsymbol{r}_1, \boldsymbol{r}_2$	=	position vectors from C to C_1 and m_2, respectively
xyz	=	body-fixed frame having its origin at C_1
β, β_d	=	resonant and detuned frequencies
ε	=	nondimensional small parameter
θ, ψ	=	generalized coordinates of the pendulum
θ_s, ϑ	=	stationary point of θ and variation from that point
μ	=	ratio of m_2 to the total mass, $m_1 + m_2$
σ	=	parameter describing the nearness of the detuned frequency to the resonance frequency
τ	=	scaled time
Φ	=	angle of rotation of the main body
$\boldsymbol{\omega}$	=	angular velocity of the coordinate system xyz

Introduction

THE attitude stability of a spin-stabilized thrusting spacecraft with internal mass motion has been studied for a long time. Numerous studies have analyzed coning instabilities of space vehicles, such as the Payload Assist Module and Delta Class upper stages, and based on the analyses of telemetries, several mechanisms have been proposed to account for the instability of a spinning spacecraft. After much speculation, the list has been narrowed to several leading destabilizing mechanisms. One of these is the liquid pool theory based on mechanical and fluid interaction.[1–4] Most studies based on this theory adopted rotor-pendulum models to describe the mechanical and fluid interaction and tried to show the appropriateness and usefulness of the proposed physical and mathematical models to explain the observed motion. Accordingly, many analyses were done for fixed parameters, that is, real flown vehicle data rather than for a wider parameter space. However, for the design and manufacture of new vehicles, it is important to do an analysis for a wider parameter range. With consideration of such aspects, a closer look is taken at the stability of internal mass motion over a wider range of parameters. Because this study is complementary to previous work,[4] it uses the same physical and mathematical models. To determine the stable–unstable regions of the internal mass motion of a spinning space vehicle, a Strutt diagram is constructed by using an analytical method. Furthermore, numerical simulations are performed at various points in the unstable and stable regions of the stability diagram to verify the analytical results. Because the internal mass in the spinning body has a motion with a periodically time-dependent coefficient and is subject to periodic external excitation, the multiple scales method is used to solve the system.

Stability Analysis of Internal Mass Motion

Stationary Solution

The spinning main body containing a liquid pool as shown in Fig. 1 has mass m_1 and centroidal principal moments of inertia, $I_1 = I_2 > I_3$, about the axes x, y, and z, respectively. The pendulum that represents a liquid mass consists of a point mass m_2 attached to a rigid massless rod, which in turn is attached at a point $\boldsymbol{O}$ to the main body, and its motion with respect to the body m_1 is defined by the angles θ and ψ. Here $\boldsymbol{r}_O$ is the position vector from C_1 to $\boldsymbol{O}$ and $\boldsymbol{r} = r(-\sin\theta\sin\psi \quad \sin\theta\cos\psi \quad -\cos\theta)^T$, which is obtained by using the 3–1 rotation sequence and the inverse transformation. For simplification, we assume that the position vector $\boldsymbol{r}_O$ and the thrust vector $\boldsymbol{F}$ align with the z axis and there is no friction torque at the

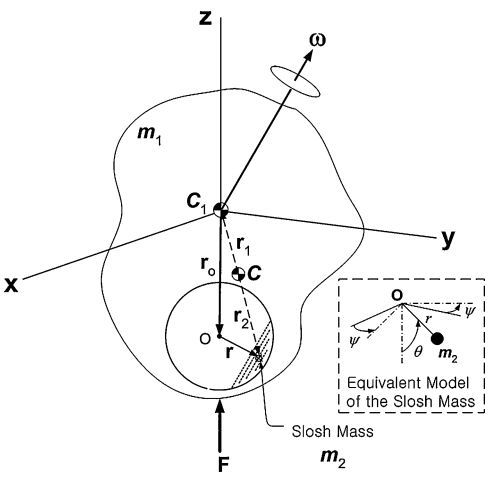

Fig. 1 Liquid pool in a spinning body.

Presented as Paper 2004-5210 at the AIAA/AAS Astrodynamics Specialist Conference, Providence, RI, 16–19 August 2004; received 22 September 2004; revision received 15 December 2004; accepted for publication 15 December 2004.

*Assistant Professor, Department of Aeronautical Science and Flight Operation, Science Hall 207, Goyang. Member AIAA.

†Professor and Head, Department of Aerospace Engineering. Associate Fellow AIAA.

pendulum hinge. Then the angular momentum vector of the system about C is $\boldsymbol{H} = (H_1 \;\; H_2 \;\; H_3)^T$. For convenience, we introduce new variables a, Φ (Ref. 5), and w such that

$$H_1 = a\sin\Phi, \qquad H_2 = a\cos\Phi, \qquad w = \psi + \Phi \tag{1}$$

where a is the transverse angular momentum component and rotates at the relative spin rate

$$\dot{\Phi} = (1 - I_3/I_1)H_3/I_3 + \mathcal{O}(\varepsilon) \tag{2}$$

From the flight data of RCA-C′ upper-stage spacecraft (Fig. 1 in Ref. 4), we observed that the spin rate changed only 12% (varied from 65 to 65.8 rpm) during the last 30 min before the attitude destabilization occurs. This means that the angular rate about the spin axis is almost constant. Therefore, we can assume that both the spacecraft and pendulum are in states of quasi-steady spin about the symmetry axis of the spacecraft. Thus, the following approximate equation for θ is obtained[4]:

$$\begin{aligned}\ddot{\theta} = {} & \left\{\left[P^2 + \mu(F_3 r_o/I_1) - \left(a^2/2I_1^2\right)(1+\cos 2w)\right]\cos\theta \right.\\ & - (F_3/m_1 r)\left[1 - \mu\left(m_1 r^2/I_1\right)\right] - a^2 r_o/I_1^2 r\Big\}\sin\theta \\ & + \left(aH_3/I_1^2\right)[1 + (r_o/r)\cos\theta]\cos w - (2aP/I_1)\sin^2\theta\cos w\end{aligned} \tag{3}$$

where $P = (\dot{\psi} + H_3/I_3)$.

At the beginning of thrusting or in a nonresonance case, a is relatively small so that the following stationary solution of θ may be obtained:

$$\begin{aligned}\theta_s = {} & \cos^{-1}\left(F_3/m_1 r P^2\right)\left\{1 - \varepsilon\left[1 + \left(F_3/m_1 r P^2\right)(r_o/r)\right]\right. \\ & \left. + \varepsilon^2\left(F_3/m_1 r P^2\right)(r_o/r)\cdots\right\}\end{aligned} \tag{4}$$

where $\varepsilon = m_1 m_2 r^2/[(m_1+m_2)I_1] = \mu m_1 r^2/I_1$. Because m_2 is very small compared with m_1 and $m_1 + m_2 \approx m_1$, ε is approximately equal to the ratio of the moment of inertia of m_2 about the point O to the lateral mass moment of inertia of the main body. As seen in Eq. (4), the equilibrium points of θ are determined mainly by axial and centrifugal accelerations.

Instability Conditions

If we introduce a term ϑ that includes higher-order terms (HOT) and expand Eq. (3) about θ_s, a new equation for the pendulum motion at the stationary point is obtained as follows:

$$\begin{aligned}\ddot{\vartheta} \approx {} & -\left(\frac{F_3}{m_1 r}\cos\theta_s - P^2\cos 2\theta_s + B_1 a\cos w\right)\vartheta \\ & + B_2 a\cos w + \text{HOT} \\ = {} & -\omega_0^2\left(1 + \frac{B_1}{\omega_0^2}a\cos w\right)\vartheta + B_2 a\cos w + \text{HOT}\end{aligned} \tag{5}$$

$$B_1 = \frac{H_3 r_o\sin\theta_s}{I_1^2 r} + \frac{2P\sin 2\theta_s}{I_1}$$

$$B_2 = \frac{H_3 r_o\cos\theta_s}{I_1^2 r} + \frac{P(\cos 2\theta_s - 1)}{I_1} + \frac{H_3}{I_1^2}, \qquad \omega_0^2 = P^2\sin^2\theta_s \tag{6}$$

In a nonresonance case, $B_1 a$ and $B_2 a$ are much smaller than a. As can be observed from Eq. (5), the pendulum is subject to parametric and external excitations. In this Note, motion of the pendulum with respect to the stationary point is assumed to be small so that the HOT in ϑ are dropped from the equation.

For convenience, Eq. (5) can be rewritten in a form similar to the Mathieu equation with forcing functions as follows:

$$\vartheta'' + (\delta + 2\varepsilon\alpha_1\cos 2\tau + 2\varepsilon\alpha_2\sin 2\tau)\vartheta = \varepsilon(k_1\cos 2\tau + k_2\sin 2\tau) \tag{7}$$

where the double prime denotes $\mathrm{d}^2(\cdot)/\mathrm{d}\tau^2$ and

$$\begin{aligned} w &= \Omega t + w_0, \qquad t = (2/\Omega)\tau, \qquad \delta = 4\omega_0^2/\Omega^2 \\ \alpha_1 &= 2B_1 a\cos w_0/\left(m_1\mu r^2\Omega^2\right) \\ \alpha_2 &= -2B_1 a\sin w_0/\left(m_1\mu r^2\Omega^2\right) \\ k_1 &= 4B_2 a\cos w_0/\left(m_1\mu r^2\Omega^2\right) \\ k_2 &= -4B_2 a\sin w_0/\left(m_1\mu r^2\Omega^2\right)\end{aligned} \tag{8}$$

Equation (7) is a nonhomogeneous linear differential equation with a periodically time-dependent coefficient. If there is no parametric excitation, that is, $a = 0$, then it becomes a second-order, constant coefficient, homogeneous, linear differential equation. To find the resonance conditions for Eq. (7), we use the method of multiple scales[6] defined by

$$T_n = \varepsilon^n\tau \tag{9}$$

for $n = 0, 1, 2, \ldots$. Then, the solution for Eq. (7) can be represented by an expansion having the form

$$\begin{aligned}\vartheta(\tau;\varepsilon) = {} & \vartheta_0(T_0, T_1, T_2, \ldots) + \varepsilon\vartheta_1(T_0, T_1, T_2, \ldots) \\ & + \varepsilon^2\vartheta_2(T_0, T_1, T_2, \ldots) + \cdots\end{aligned} \tag{10}$$

By carrying out the expansion to the order of ε^2 and equating the coefficients of equal powers of ε, one may find the following equations:

$$D_0^2\vartheta_0 + \delta\vartheta_0 = 0 \tag{11}$$

$$\begin{aligned}D_0^2\vartheta_1 + \delta\vartheta_1 = {} & -2D_0 D_1\vartheta_0 - 2\alpha_1\vartheta_0\cos 2T_0 - 2\alpha_2\vartheta_0\sin 2T_0 \\ & + k_1\cos 2T_0 + k_2\sin 2T_0\end{aligned} \tag{12}$$

$$\begin{aligned}D_0^2\vartheta_2 + \delta\vartheta_2 = {} & -2D_0 D_2\vartheta_0 - D_1^2\vartheta_0 - 2D_0 D_1\vartheta_1 \\ & - 2\alpha_1\vartheta_1\cos 2T_0 - 2\alpha_2\vartheta_1\sin 2T_0\end{aligned} \tag{13}$$

where

$$D_0 = \frac{\partial}{\partial T_0}, \qquad D_1 = \frac{\partial}{\partial T_1}, \qquad D_2 = \frac{\partial}{\partial T_2}, \ldots, D_i = \frac{\partial}{\partial T_i}\cdots \tag{14}$$

The general solution to Eq. (11) can be written in the form

$$\vartheta_0 = A(T_1, T_2)e^{i\beta T_0} + \bar{A}(T_1, T_2)e^{-i\beta T_0} \tag{15}$$

where $\beta = \delta^{1/2}$ and $\bar{A}$ is the complex conjugate (CC) of A. Then, Eq. (12) may be written as

$$\begin{aligned}D_0^2\vartheta_1 + \beta^2\vartheta_1 = {} & -2i\beta D_1 A e^{i\beta T_0} - (\alpha_1 - i\alpha_2)A e^{i(2+\beta)T_0} \\ & - (\alpha_1 - i\alpha_2)\bar{A}e^{i(2-\beta)T_0} + \tfrac{1}{2}(k_1 - ik_2)e^{i2T_0} + \text{CC}\end{aligned} \tag{16}$$

Because the behavior of the motion near resonance is of concern, a detuning parameter σ can be introduced such that

$$\beta_d = \beta + \varepsilon\sigma \tag{17}$$

where β_d denotes a detuned frequency. The parameter σ allows one to describe the nearness of the detuned frequency to the resonant frequency and helps one recognize the terms in the governing equation for ϑ_1 that lead to secular or nearly secular terms. By analyzing the particular solutions of Eq. (16), one may find many resonance conditions. However, we will confine our analysis to finite cases that are realistic to the actual system and, thus, construct the corresponding stability diagram by considering only four cases, $\beta \approx 0$, 1, 2, and 4.

Stability Diagram

The stability transition curves used to construct a stability diagram are summarized in Table 1 and the derivation of the curves is given in the Appendix. The underlying idea of the method of multiple scales is introduced in Ref. 6.

Figure 2 is a Strutt diagram for Eq. (3) where the solid lines represent loci of transition values that separate the $\varepsilon\alpha$–δ plane into regions of stability and instability. The shaded area represents the unstable region, and the unshaded area represents the stable region. However, because the actual system uses particular values of its design parameters, no more than one resonance case occurs in the system.

For an application of the preceding analyses results, we consider a spacecraft with the following parameters: $F_3 = 71171.6$ N, $m_1 = 1950.5$ kg, $m_2 = 4.4$ kg, $I_1 = I_2 = 1831.1$ kg·m^2, $I_3 = 623.9$ kg·m^2, $r_o = 1.0$ m, $r = 0.6$ m, $a = 27.12$ kg·m^2/s, and $\omega_3 = 52.4$ rpm.

To verify the analytical results, numerical simulations were conducted for various points in the parameter plane of Fig. 2. Time histories of θ for parameter combinations corresponding to various points in the parameter plane of Fig. 2 are shown in Figs. 3–14. Figures 3–10 show two possible types of unbounded solutions. The first type is nonoscillatory and increases exponentially with time (Figs. 3 and 4), whereas the second type is oscillatory but with amplitude that increases exponentially with time (Figs. 5–10). The points in the band of case 1 including P_1 and P_2 correspond to the first type, and the points in the other unstable bands correspond to the second type. The amplitude of the time response corresponding to point P_7 has a very small growth rate (Fig. 9). Also, as can be expected, the unstable time responses grow more rapidly as the value of $\varepsilon\alpha$ increases.

The bounded solutions corresponding to points P_9–P_{12} are shown in Figs. 11–14. They are aperiodic and vary with the frequency composed of the main and parametric excitation frequencies.

Table 1 Stability transition curves

Case	Transition curve
$\beta \approx 0$	$\delta = -\frac{1}{2}\varepsilon^2\alpha^2 + \mathcal{O}(\varepsilon^3)$
$\beta \approx 1$	$\delta = 1 \pm \varepsilon\alpha + \frac{3}{8}\varepsilon^2\alpha^2 \pm \frac{1}{8}\varepsilon^3\alpha^3 + \mathcal{O}(\varepsilon^4)$
$\beta \approx 2$	$\delta = 4 + (5/12)\varepsilon^2\alpha^2 + \mathcal{O}(\varepsilon^3)$ and $\delta = 4 - (1/12)\varepsilon^2\alpha^2 + \mathcal{O}(\varepsilon^3)$
$\beta \approx 4$	$\delta = 16 + (1/30)\varepsilon^2\alpha^2 + \mathcal{O}(\varepsilon^4)$

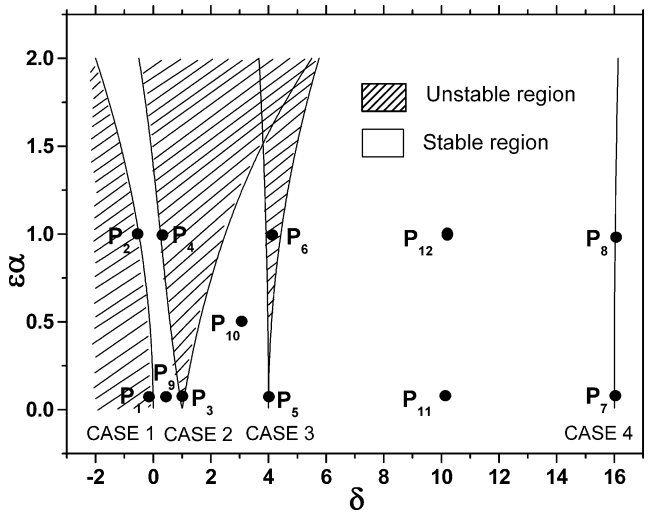

Fig. 2 Strutt diagram.

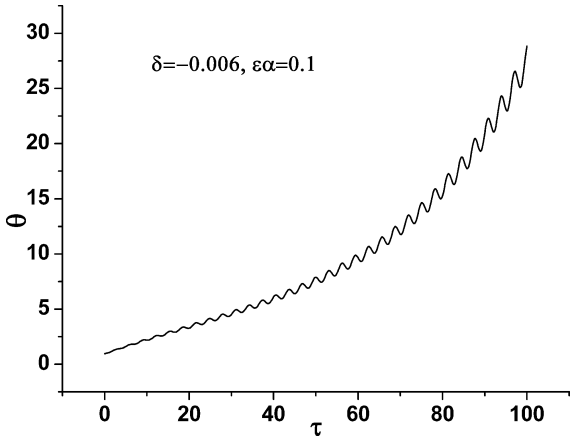

Fig. 3 Time history of θ at P_1.

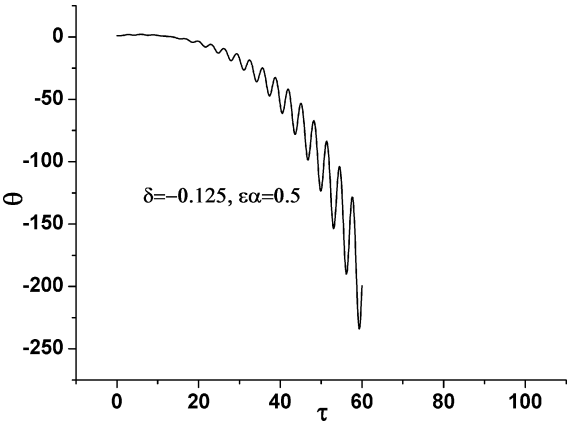

Fig. 4 Time history of θ at P_2.

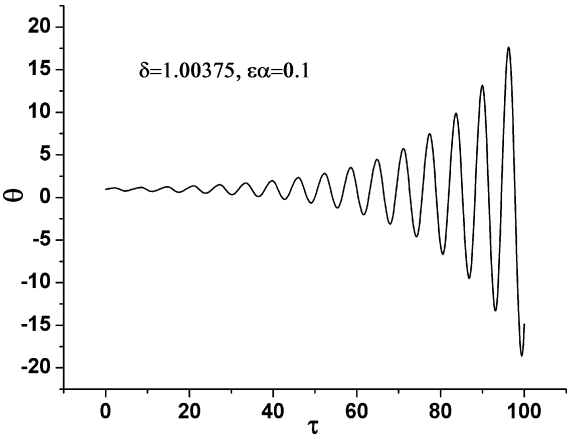

Fig. 5 Time history of θ at P_3.

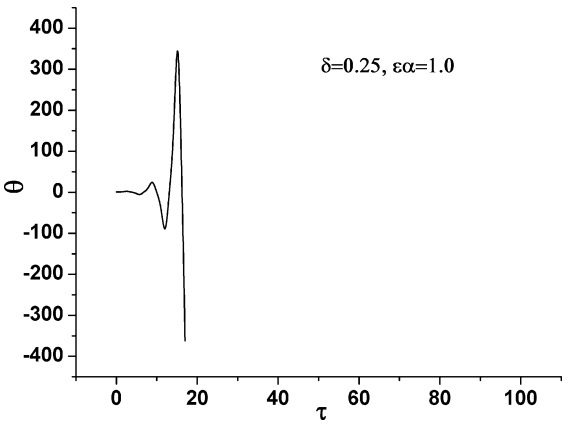

Fig. 6 Time history of θ at P_4.

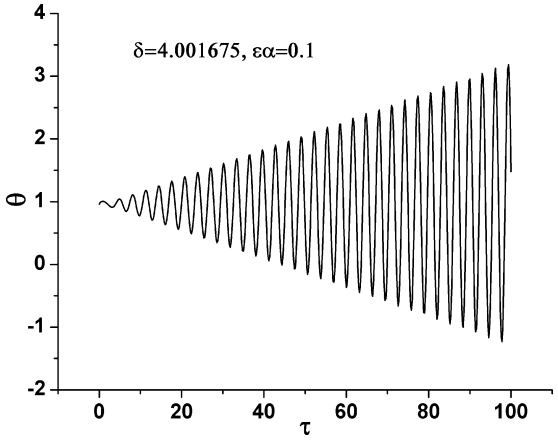

Fig. 7 Time history of θ at P_5.

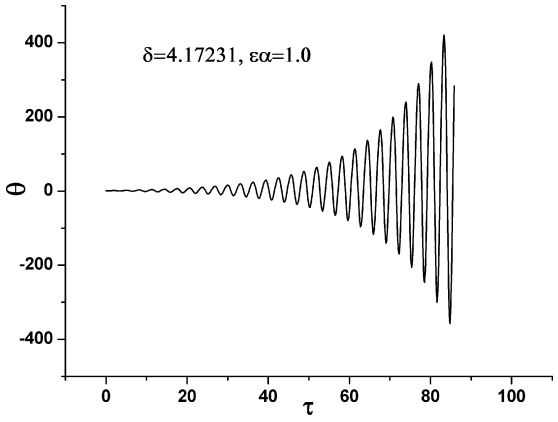

Fig. 8 Time history of θ at P_6.

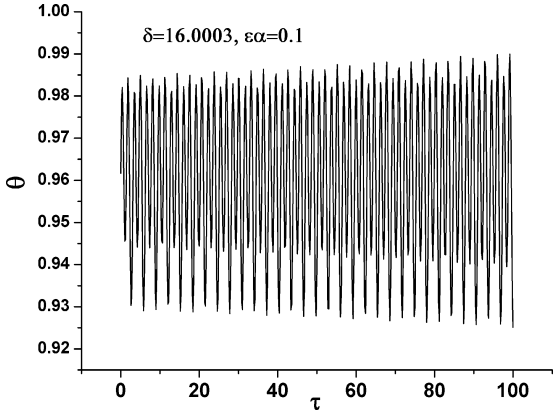

Fig. 9 Time history of θ at P_7.

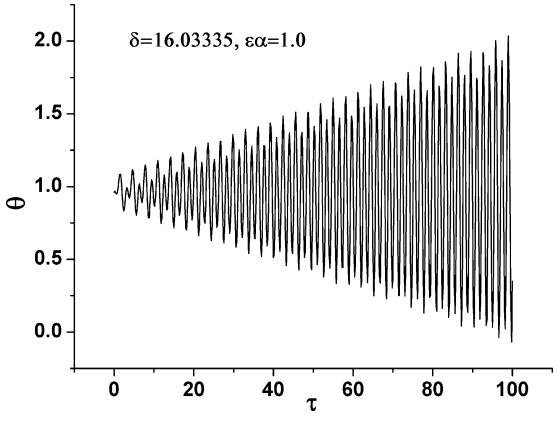

Fig. 10 Time history of θ at P_8.

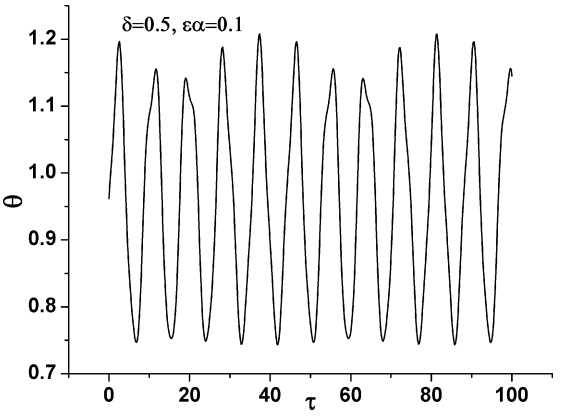

Fig. 11 Time history of θ at P_9.

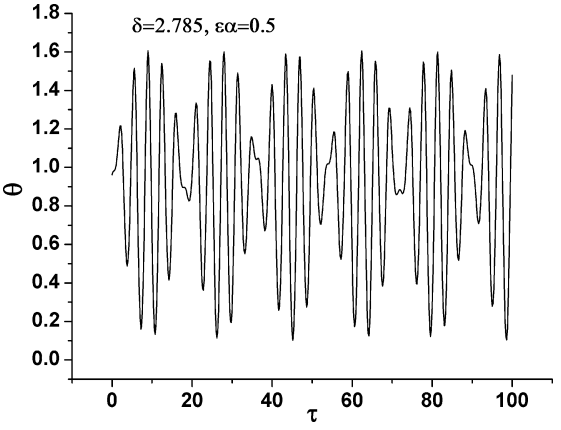

Fig. 12 Time history of θ at P_{10}.

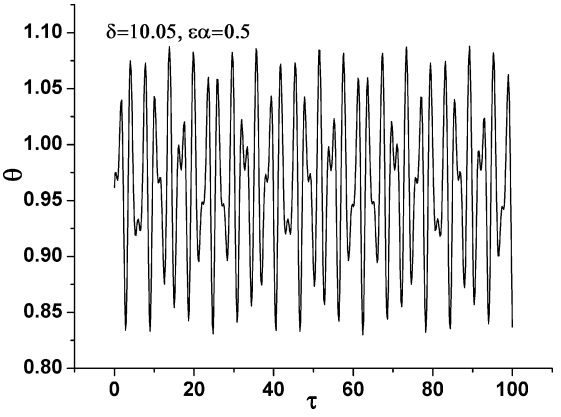

Fig. 13 Time history of θ at P_{11}.

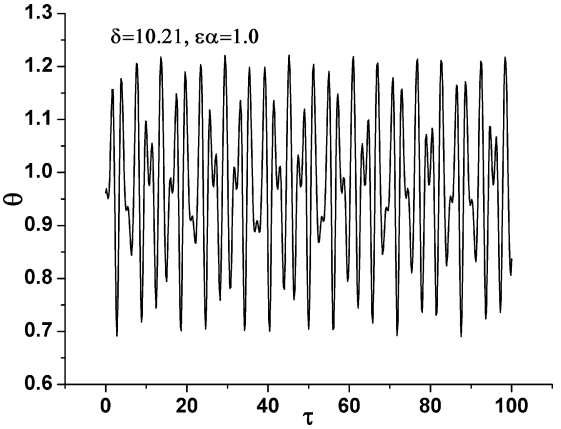

Fig. 14 Time history of θ at P_{12}.

Conclusions

As an extension of previous work, the dynamic stability of the internal mass of a spinning vehicle was investigated for a wider parameter space. To provide suitable design criteria for a broader applicability to the class of spinning spacecraft, the same physical and mathematical models were used. Because the behavior of motion near resonance was of concern, four probable resonant conditions and corresponding stability transition curves were derived by an analytical method. By using these curves, we constructed a Strutt diagram. The locus of transition values in the diagram separates the $\varepsilon\alpha$–δ plane into regions of stability and instability. Therefore, stable–unstable regions of the internal mass motion of the spinning vehicle in terms of parameters can be determined easily. Sometimes it may be hard to interpret directly the final results for the actual application because many physical parameters are combined into a single parameter or several parameters. However, it is possible to interpret the results if we make and use a computer program that calculates the relationship between parameters. For example, plugging basic data (parameters) of the spacecraft into the program, we will get a point in the parameter plane of the Strutt diagram. If the point appears in the unstable region, we can change the values of some design parameters and repeat these steps until the point appears in the desired stable region.

To verify the analytical results of the stability, numerical simulations were performed using the basic data of the spacecraft and parameter values corresponding to the points in the Strutt diagram. Simulation results for each point in the parameter plane show that characteristics of the stability of motion are as expected, and thus, the analytically obtained stability diagram is appropriate. Time histories of the pendulum motion at the points in the unstable band emanating from $\beta = 0$ are nonoscillatory and increase exponentially with time, whereas those corresponding to points in other unstable bands (emanating from $\beta = 1$, 2, and 4) are oscillatory but with amplitudes that increase mostly exponentially with time. Because the previous study[4] showed that the slosh mass serves as an energy storage and generates disturbance torques about the pitch and yaw axis of the main body, it is important that the parameter combinations should remain in the stable regions of the Strutt diagram.

Appendix: Derivation of Stability Transition Curves

Case $\beta \approx 0$

In this case we let

$$\delta = \varepsilon\sigma_1 + \varepsilon^2\sigma_2 + \cdots \tag{A1}$$

Then Eqs. (12–14) can be rewritten as

$$D_0^2\vartheta_0 = 0 \tag{A2}$$

$$D_0^2\vartheta_1 = -\sigma_1\vartheta_0 - 2D_0D_1\vartheta_0 - 2\alpha_1\vartheta_0\cos 2T_0 - 2\alpha_2\vartheta_0\sin 2T_0 + k_1\cos 2T_0 + k_2\sin 2T_0 \tag{A3}$$

$$D_0^2\vartheta_2 = -\sigma_2\vartheta_0 - \sigma_1\vartheta_1 - 2D_0D_2\vartheta_0 - D_1^2\vartheta_0 - 2D_0D_1\vartheta_1 - 2\alpha_1\vartheta_1\cos 2T_0 - 2\alpha_2\vartheta_1\sin 2T_0 \tag{A4}$$

The solution of Eq. (A2) can be expressed as

$$\vartheta_0 = A(T_1, T_2) \tag{A5}$$

Then Eq. (A3) becomes

$$D_0^2\vartheta_1 = -(\sigma_1 + 2\alpha_1\cos 2T_0 + 2\alpha_2\sin 2T_0)A + k_1\cos 2T_0 + k_2\sin 2T_0 \tag{A6}$$

Eliminating secular terms from ϑ_1 requires that $\sigma_1 = 0$. Then when the homogeneous solution is disregarded, the solution for Eq. (A6) becomes

$$\vartheta_1 = -\tfrac{1}{2}\left(\alpha_1 A - \tfrac{1}{8}k_1\right)\cos 2T_0 + \tfrac{1}{2}\left(\alpha_2 A - \tfrac{1}{8}k_2\right)\sin 2T_0 \tag{A7}$$

Then Eq. (A4) becomes

$$D_0^2\vartheta_2 = -\sigma_2 A - D_1^2 A - \tfrac{1}{2}\left(\alpha_1^2 + \alpha_2^2\right)A + \tfrac{1}{2}(\alpha_1K_1 + \alpha_2k_2) + 2D_1A(\alpha_1\sin 2T_0 - \alpha_2\cos 2T_0) - \tfrac{1}{2}\left[\left(\alpha_1^2 - \alpha_2^2\right)A - \tfrac{1}{2}(\alpha_1k_1 - \alpha_1k_1)\right]\cos 4T_0 - \tfrac{1}{2}\left[2\alpha_1\alpha_2 A - \tfrac{1}{2}(\alpha_1k_2 + \alpha_2k_1)\right]\sin 4T_0 \tag{A8}$$

Eliminating the secular terms from ϑ_2 requires that

$$D_1^2 A + \left[\sigma_2 + \tfrac{1}{2}\left(\alpha_1^2 + \alpha_2^2\right)\right]A - \tfrac{1}{2}(\alpha_1k_1 + \alpha_2k_2) = 0 \tag{A9}$$

from which we get

$$A = a_1\exp\left[i\sqrt{\sigma_2 + \tfrac{1}{2}\left(\alpha_1^2 + \alpha_2^2\right)}T\right] + a_2\exp\left[-i\sqrt{\sigma_2 + \tfrac{1}{2}\left(\alpha_1^2 + \alpha_2^2\right)}T\right] + \frac{1}{2}\frac{(\alpha_1k_1 + \alpha_2k_2)}{\sigma_2 + \tfrac{1}{2}\left(\alpha_1^2 + \alpha_2^2\right)} \tag{A10}$$

Therefore, ϑ is bounded if $\sigma_2 \geq -\frac{1}{2}(\alpha_1^2 + \alpha_2^2)$ and unbounded if $\sigma_2 < -\frac{1}{2}(\alpha_1^2 + \alpha_2^2)$. Consequently, $\sigma_2 = -\frac{1}{2}(\alpha_1^2 + \alpha_2^2)$ separates the stable from the unstable solution, and the transition curve emanating from $\delta \approx 0$ becomes

$$\delta = -\tfrac{1}{2}\varepsilon^2\alpha^2 + \mathcal{O}(\varepsilon^3) \tag{A11}$$

Case $\beta \approx 1$

In this case, the particular solution becomes

$$\vartheta_1 = [1/4(\beta+1)]\{(\alpha_1 - i\alpha_2)A\exp[i(2+\beta)T_0] + (\alpha_1 + i\alpha_2)\bar{A}\exp[-i(2+\beta)T_0]\} + [1/2(\beta^2-4)] \times [(k_1 - ik_2)\exp(i2T_0) + (k_1 + i\alpha_2)\exp(-i2T_0)] \tag{A12}$$

Because $\beta = 1 - \varepsilon\sigma$, the detuning parameters and transition curves emanating from $\delta \approx 1$ correspond to

$$\sigma = \mp\tfrac{1}{2}\alpha - (1/16)\varepsilon\alpha^2 \mp (1/32)\varepsilon^2\alpha^3 + \mathcal{O}(\varepsilon^3) \tag{A13}$$

$$\delta = 1 \pm \varepsilon\alpha + \tfrac{3}{8}\varepsilon^2\alpha^2 \pm \tfrac{1}{8}\varepsilon^3\alpha^3 + \mathcal{O}(\varepsilon^4) \tag{A14}$$

Case $\beta \approx 2$

Similarly, we can proceed further to $\beta \approx 2$ to obtain the particular solution

$$\vartheta_1 = [1/4(\beta+1)]\{(\alpha_1 - i\alpha_2)A\exp[i(2+\beta)T_0] + (\alpha_1 + i\alpha_2)\bar{A}\exp[-i(2+\beta)T_0]\} - [1/4(\beta-1)]\{(\alpha_1 - i\alpha_2)\bar{A}\exp[i(2-\beta)T_0] + (\alpha_1 + i\alpha_2)A\exp[-i(2-\beta)T_0]\} \tag{A15}$$

Because $2 = \beta + \varepsilon\sigma$, the detuning parameters correspond to

$$\sigma = -\varepsilon(5/48)\left(\alpha_1^2 + \alpha_2^2\right) + \mathcal{O}(\varepsilon^2)$$

$$\sigma = \varepsilon(1/48)\left(\alpha_1^2 + \alpha_2^2\right) + \mathcal{O}(\varepsilon^2) \tag{A16}$$

Hence, the transition curves emanating from $\delta \approx 4$ are given by

$$\delta = 4 + (5/12)\varepsilon^2\alpha^2 + \mathcal{O}(\varepsilon^3), \qquad \delta = 4 - (1/12)\varepsilon^2\alpha^2 + \mathcal{O}(\varepsilon^3) \tag{A17}$$

Case $\beta \approx 4$

Eliminating the terms that produce secular terms in Eq. (16) leads to $D_1 A = 0$ so that $A = A(T_2)$. Hence, the particular solution of Eq. (16) is

$$\begin{aligned}\vartheta_1 &= [1/4(\beta+1)]\{(\alpha_1 - i\alpha_2)A\exp[i(2+\beta)T_0] \\ &\quad + (\alpha_1 + i\alpha_2)\bar{A}\exp[-i(2+\beta)T_0]\} \\ &\quad - [1/4(\beta-1)]\{(\alpha_1 - i\alpha_2)\bar{A}\exp[i(2-\beta)T_0] \\ &\quad + (\alpha_1 + i\alpha_2)A\exp[-i(2-\beta)T_0]\} \\ &\quad + [1/2(\beta^2-4)][(k_1 - ik_2)\exp(i2T_0) \\ &\quad + (k_1 + ik_2)\exp(-i2T_0)] \end{aligned} \tag{A18}$$

Substituting for ϑ_0 and ϑ_1 into Eq. (13) yields

$$\begin{aligned} D_0^2\vartheta_2 + \delta\vartheta_2 &= -2i\beta D_2 A\exp(i\beta T_0) - \frac{\alpha_1(\alpha_1 - i\alpha_2)}{4(\beta+1)} \\ &\quad \times A\{\exp[i(4+\beta)T_0] + \exp(i\beta T_0)\} \\ &\quad + \frac{\alpha_1}{4(\beta-1)}\{(\alpha_1 - i\alpha_2)\bar{A}\exp[i(4-\beta)T_0] \\ &\quad + (\alpha_1 + i\alpha_2)A\exp(i\beta T_0)\} \\ &\quad - \frac{\alpha_1}{2(\beta^2-4)}[(k_1 - ik_2)\exp(i4T_0) + (k_1 - ik_2)] \\ &\quad + i\frac{\alpha_2(\alpha_1 - i\alpha_2)}{4(\beta+1)}A\{\exp[i(4+\beta)T_0] - \exp(i\beta T_0)\} \\ &\quad - i\frac{\alpha_2}{4(\beta-1)}\{(\alpha_1 - i\alpha_2)\bar{A}\exp[i(4-\beta)T_0] \\ &\quad + (\alpha_1 + i\alpha_2)A\exp(i\beta T_0)\} + i\frac{\alpha_2}{2(\beta^2-4)} \\ &\quad \times [(k_1 - ik_2)\exp(i4T_0) + (k_1 + ik_2)] + \text{CC} \end{aligned} \tag{A19}$$

Elimination of terms that produce secular terms from Eq. (19) yields

$$2\beta D_2 A - i\left[\frac{\alpha_1^2 + \alpha_2^2}{4(\beta^2-1)}\right]A = 0 \tag{A20}$$

The solutions for A and $\bar{A}$ are

$$\begin{aligned} A &= A_0\exp\left\{-i\left[\frac{\alpha_1^2+\alpha_2^2}{4\beta(\beta^2-1)}T_2 - C_0\right]\right\} \\ \bar{A} &= A_0\exp\left\{i\left[\frac{\alpha_1^2+\alpha_2^2}{4\beta(\beta^2-1)}T_2 - C_0\right]\right\} \end{aligned} \tag{A21}$$

Therefore, the solution of the system is

$$\begin{aligned}\vartheta &= \vartheta_0 + \varepsilon\vartheta_1 + \mathcal{O}(\varepsilon^2) \\ &= a_0\cos\varphi + \varepsilon[a_0/4(\beta+1)] \\ &\quad \times [\alpha_1\cos(2T_0+\varphi) + \alpha_2\sin(2T_0+\varphi)] \\ &\quad - \varepsilon[a_0/4(\beta-1)][\alpha_1\cos(2T_0-\varphi) + \alpha_2\sin(2T_0-\varphi)] \\ &\quad + \varepsilon[1/(\beta^2-4)][k_1\cos(2T_0) + k_2\sin(2T_0)] + \mathcal{O}(\varepsilon^2) \end{aligned} \tag{A22}$$

where

$$a_0 = 2A_0, \qquad \varphi = \left[\beta - \varepsilon^2\frac{\alpha_1^2+\alpha_2^2}{4\beta(\beta^2-1)}\right]T_0 + C_0 \tag{A23}$$

When $\beta \approx 4$, we introduce a detuning parameter σ defined by

$$4 = \beta + \varepsilon^2\sigma \tag{A24}$$

and express $4T_0$ from Eq. (A19) as $4T_0 = \beta T_0 + \sigma T_2$. Then, elimination of the terms that produce secular terms in Eq. (A19) gives

$$\begin{aligned} D_2 A + i\frac{\alpha_1^2+\alpha_2^2}{4\beta(\beta^2-1)}A \\ - \frac{(\alpha_1 k_2 + \alpha_2 k_1) + i(\alpha_1 k_1 - \alpha_2 k_2)}{4\beta(\beta^2-4)}e^{i\sigma T_2} = 0 \end{aligned} \tag{A25}$$

Let

$$A = (A_r + iA_i)e^{i\sigma T_2} \tag{A26}$$

where A_r and A_i are real. Putting this into Eq. (A25) and separating the real and imaginary parts, we get

$$D_2 A_r - \sigma_s A_i = f_1, \qquad D_2 A_i + \sigma_s A_r = f_2 \tag{A27}$$

where

$$\begin{aligned} \sigma_s &= \sigma + \frac{\alpha_1^2+\alpha_2^2}{4\beta(\beta^2-1)}, \qquad f_1 = \frac{\alpha_1 k_2 + \alpha_2 k_1}{4\beta(\beta^2-4)} \\ f_2 &= \frac{\alpha_1 k_1 - \alpha_2 k_2}{4\beta(\beta^2-4)} \end{aligned} \tag{A28}$$

When σ_s is not zero, Eq. (A27) admits a general solution in the form

$$A_r = a_r e^{\gamma T_2} + a_{r0}, \qquad A_i = a_i e^{\gamma T_2} + a_{i0} \tag{A29}$$

where a_r, a_{r0}, a_i, and a_{i0} are constants, provided that

$$\gamma^2 = -\sigma_s^2 \tag{A30}$$

$$a_{r0} = f_2/\sigma_s, \qquad a_{i0} = -f_1/\sigma_s \tag{A31}$$

Equations (A29) become

$$\begin{aligned} A_r &= a_1\cos(\sigma_s T_2) + a_2\sin(\sigma_s T_2) + f_2/\sigma_s \\ A_i &= -a_1\sin(\sigma_s T_2) + a_2\cos(\sigma_s T_2) - f_1/\sigma_s \end{aligned} \tag{A32}$$

where a_1 and a_2 are constants.

If σ_s is zero, that is, $\sigma = -(\alpha_1^2+\alpha_2^2)/4\beta(\beta^2-4)$, Eq. (A27) has a solution in the form $A_r = f_1 T_2 + a_{r0}$ and $A_i = f_2 T_2 + a_{i0}$. Hence, Eq. (A26) becomes

$$\begin{aligned} A = \left\{\left[\frac{\alpha_1 k_2 + \alpha_2 k_1}{4\beta(\beta^2-4)} + i\frac{\alpha_1 k_1 + \alpha_2 k_2}{4\beta(\beta^2-4)}\right]T_2 + (a_{r0} + ia_{i0})\right\} \\ \times \exp\left[-i\frac{\alpha_1^2+\alpha_2^2}{4\beta(\beta^2-1)}T_2\right] \end{aligned} \tag{A33}$$

which grows with time. The transition curve emanating from $\beta \approx 4$ is

$$\delta = 16 + (1/30)\varepsilon^2\alpha^2 + \mathcal{O}(\varepsilon^4), \qquad \alpha = \sqrt{\alpha_1^2+\alpha_2^2} \tag{A34}$$

References

[1] Or, A. C., and Challoner, A. D., "Stability of Spinning Spacecraft Containing Shallow Pool of Liquid Under Thrust," *Journal of Guidance, Control, and Dynamics*, Vol. 17, No. 5, 1994, pp. 1019–1027.

[2] Meyer, R. X., "Coning Instability of Spacecraft During Periods of Thrust," *Journal of Spacecraft and Rockets*, Vol. 33, No. 6, 1996, pp. 781–788.

[3] Yam, Y., Mingori, D. L., and Halsmer, D. M., "Stability of a Spinning Axisymmetric Rocket with Dissipative Internal Mass Motion," *Journal of Guidance, Control, and Dynamics*, Vol. 20, No. 2, 1997, pp. 306–312.

[4] Kang, J. Y., and Cochran, J. E., Jr., "Resonant Motion of a Spin-Stabilized Thrusting Spacecraft," *Journal of Guidance, Control, and Dynamics*, Vol. 27, No. 3, 2004, pp. 356–364.

[5] Cochran, J. E., "Nonlinear Resonances in the Attitude Motion of Dual-Spin Spacecraft," *Journal of Spacecraft and Rockets*, Vol. 14, No. 9, 1977, pp. 562–572.

[6] Nayfeh, A. H., and Mook, D. T., *Nonlinear Oscillations*, Wiley, New York, 1979, pp. 56–59.